

Article

Seismic Data Interpretation and Identification of Hydrocarbon-Bearing Zones of Rajian Area, Pakistan

Naveed Ahmad ¹, Sikandar Khan ^{2,*}, Eisha Fatima Noor ³, Zhihui Zou ⁴ and Abdullatif Al-Shuhail ⁵

¹ Department of Marine Geophysics, Ocean University of China, Qingdao 266100, China; naveedahmadgeophy@gmail.com

² Department of Mechanical Engineering, King Fahd University of Petroleum and Minerals, Dhahran 31261, Saudi Arabia

³ Department of Earth and Environmental Sciences, Bahria University Islamabad, Islamabad 44000, Pakistan; eishafatimanoor@gmail.com

⁴ Department of Geodetection and Information Technology, College of Marine Geosciences, Ocean University of China, Qingdao 266100, China; zouzhihui@ouc.edu.cn

⁵ Department of Geosciences, King Fahd University of Petroleum and Minerals, Dhahran 31261, Saudi Arabia; ashuhail@kfupm.edu.sa

* Correspondence: sikandarkhan@kfupm.edu.sa

Abstract: The present study interprets the subsurface structure of the Rajian area using seismic sections and the identification of hydrocarbon-bearing zones using petrophysical analysis. The Rajian area lies within the Upper Indus Basin in the southeast (SE) of the Salt Range Potwar Foreland Basin. The marked horizons are identified using formation tops from two vertical wells. Seismic interpretation of the given 2D seismic data reveals that the study area has undergone severe distortion illustrated by thrusts and back thrusts, forming a triangular zone within the subsurface. The final trend of those structures is northwest–southeast (NW–SE), indicating that the area is part of the compressional regime. The zones interpreted by the study of hydrocarbon potential include Sakessar limestone and Khewra sandstone. Due to the unavailability of a petrophysics log within the desired investigation depths, lithology cross-plots were used for the identification of two potential hydrocarbon-bearing zones in one well at depths of 3740–3835 m (zone 1) and 4015–4100 m (zone 2). The results show that zone 2 is almost devoid of hydrocarbons, while zone 1 has an average hydrocarbon saturation of about 11%.

Keywords: subsurface structural interpretation; contour mapping; hydrocarbon-bearing zones; petrophysical analysis



check for updates

Citation: Ahmad, N.; Khan, S.; Noor, E.F.; Zou, Z.; Al-Shuhail, A. Seismic Data Interpretation and Identification of Hydrocarbon-Bearing Zones of Rajian Area, Pakistan. *Minerals* **2021**, *11*, 891. <https://doi.org/10.3390/min11080891>

Academic Editors: Monika Ivandic and Fengjiao Zhang

Received: 8 June 2021

Accepted: 16 August 2021

Published: 18 August 2021

Publisher's Note: MDPI stays neutral with regard to jurisdictional claims in published maps and institutional affiliations.



Copyright: © 2021 by the authors. Licensee MDPI, Basel, Switzerland. This article is an open access article distributed under the terms and conditions of the Creative Commons Attribution (CC BY) license (<https://creativecommons.org/licenses/by/4.0/>).

1. Introduction

The main task of seismic interpretation is to characterize underground geological structures and lithology with high precision. Seismic data analysis can distinguish between rocks that contain hydrocarbons and rocks that do not contain hydrocarbons. In contrast, it is difficult to distinguish between payable oil and gas intervals and non-payable oil and gas intervals just by interpreting seismic data [1–3]. Several strategies have been widely used in seismic description, notably, seismic attributes, petrophysical models, and fluid saturation. Increased water saturation is the main reason for the development of well failure. The water saturation information obtained from seismic data is somewhat complex if petrophysical modeling methods are not used. Fluid substitution in well data provides tools for the identification and quantification of fluids in reservoirs [4,5].

Seismic structural interpretation involves highlighting and extracting faults and horizons that are apparent as geometric features in a seismic image. Seismic image processing methods have been proposed to automate fault and horizon interpretation, each of which today still requires significant human effort. Velocity modeling is highly dependent upon input from geological and petrophysical data and interpretations. Faults and horizons are

the most important structural mappings that can be extracted from a 3D seismic image. In a seismic image, interpreters laterally track geologically consistent reflections to extract horizons while identifying reflection discontinuities to pick faults. Measuring reflection discontinuity alone is insufficient to distinguish faults from other discontinuous features such as noise and stratigraphic features [6].

The expedition to survey hydrocarbons in Pakistan began in 1868, when the first drilling operation was performed at Kundal near Mianwali. The first oil discovery was made in 1915, with the drill of Khaur-01. The majority of the rocks in Pakistan are sedimentary and are rich in petroliferous content. The main goal of petroleum companies is to identify structural and stratigraphic traps where the potential of hydrocarbon accumulation is high. In Pakistan, these structures are present in areas of strong folding and faulting, i.e., the Potwar area [7].

The analysis and interpretation of geophysical data provide an understanding of the structural geology of the Gorgan plain, which is crucial for the investigation of structural traps. Seismic interpretation indicates structural features, such as deep reverse listric faults (inverted normal faults) for older formations; strike-slip and normal faults in younger sequences; and dome and basin interference patterns of folding for all of the above formations [8].

Geophysicists have conducted petroleum exploration for a considerable amount of time, and they have developed many methods for hydrocarbon exploration. The seismic reflection technique is used for deep hydrocarbon exploration. Petroleum geologists have introduced major useful techniques for hydrocarbon exploration. Geophysical methods are used to study the earth's interior. These methods are used to take measurements at or near the earth's surface for investigation that can disclose both lateral and vertical changes in physical properties of the earth's subsurface. Logs such as electrical, nuclear, and acoustic have been used to study these subsurface changes. The carbon dioxide geological sequestration and utilization requires that the reservoir properties should be known before performing the actual injection process. The reservoir properties evaluated from the geophysical methods can be used as inputs when performing reservoir geomechanical modeling before the actual carbon dioxide injection process [9–15].

The integrated strategy optimizes well performance in an iterative manner. The integrated solution is introduced by integrating various well types of geometry and fine zonation of the target formation. The combination of each zone and each well type is based on potential oil-bearing zones predefined by well log data analysis [16].

Introducing and applying an appropriate strategy for reservoir modeling in strongly heterogeneous and fractured reservoirs is a controversial issue in reservoir engineering. Various integration approaches have been introduced to combine different sources of information and model building techniques to handle heterogeneity in geologically complex reservoirs. However, most of these integration approaches in several studies fail in terms of modeling strongly fractured limestone reservoir rocks [17].

The current study is a first attempt to perform a subsurface structural interpretation of the Rajian area using seismic sections. The identification of the hydrocarbon-bearing zones is also performed for the first time in the current study using a petrophysical analysis. The marked horizons are identified using formation tops from two vertical wells. The Rajian area is under the compressional stress regime. The lithology cross-plots are used for the identification of the potential hydrocarbon-bearing zones. Based on the current study, the zones with hydrocarbon potential include Sakessar limestone and Khewra sandstone.

2. Location and Tectonics of the Study Area

The area under study is the Rajian field, Gujar Khan, as shown in Figure 1. It is located about 60 KM SE of Islamabad. The Gujar Khan is located in the western lower region of the Himalayas in north Pakistan. The terms NPDZ and SPPZ represent Northern Potwar Deformed Zone and Southern Potwar Platform Zone, respectively. A-A' and B-B' depict cross-sections locations for the Potwar Basin in Northern Pakistan. The dotted

line represents the Soan syncline, which runs northeast-southwest direction. The Soan syncline isolates the region into less deformed Southern Potwar Platform Zone (SPPZ) and more deformed Northern Potwar Deformed Zone (NPDZ). The Potwar sub-basin is renowned for its large reserves of oil and petroleum gas and is viewed as one of the world's most established oil regions; the first oil discovery was made in Khaur (1914). Around 150 exploratory wells have been drilled in this area, but the vast majority of them are not useable today, predominantly because of the heavy-weight water in molasses stores. Rajian geographically shares its border with Islamabad and Rawalpindi in the north, and to the west lie Jhelum and Gujrat. It is easily accessible due to the development of the M2 motorway as well as the Islamabad–Lahore Grand Trunk Road [18,19].

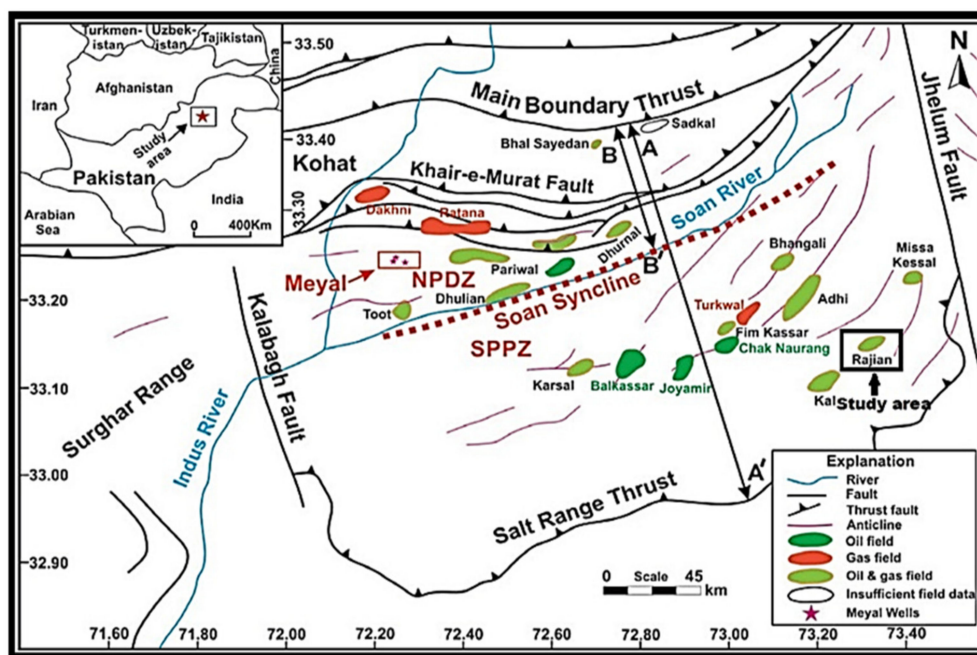


Figure 1. Regional tectonic setting of Rajian area [19].

The Potwar basin is one of the most established and old oil zones in which triangular zones are very common. In northern Pakistan, the study area is located to the west of the Himalayas. The Potwar Plateau, salt range, and Jhelum plain are in this area. Due to the collision between Indian and Eurasian plates, the Himalayan Orogenic belt came into existence. The subduction of the Indian plate decoupled the sedimentary record from the basement. The sedimentary succession has been imbricated with a broad arrangement of thrusts and nappes [20].

The Kohat–Potwar foreland basin encompasses a distorted sedimentary sequence from the Paleocene to the Pleistocene. Its northern boundary is with the Main Boundary Thrust (MBT); its southern boundary is with the Salt Range Thrust (SRT); the Kalabagh fault and Indus River are to its west; and to its east is the Jhelum fault. The portion between the Jhelum fault and Kalabagh fault is known as the Potwar sub-basin, and the area west of the Kalabagh fault between the SRT and MBT portion is known as the Kohat sub-basin. To the west of the Kalabagh fault, the range causing a bend is known as the Surghar, range and below this is the Khisor range. The ranges between the two rivers (Jhelum and Indus) are known as the Cis-Indus ranges, and the Surghar and Khisor ranges are known as the Trans-Indus Ranges [21].

The study area lies in eastern Potwar. Eastern Potwar is an area with a highly active tectonic framework composed of low-angle thrust faults with observable shortening when compared to other regions of Potwar fold. The thrust belt and faulted structures are very prominent in the area under study (Figure 1). Most of the folds in eastern Potwar

have a direction of NE–SW, and there are very few east–west (E–W) trending folds in the focal district. Imbricate thrusts, popup structures, and triangular zones are found here. Over-thrusting in the area resulted in the formation of fault-limited hydrocarbon (HC) traps. Potwar is bounded by a salt range thrust in the south. The second important thrust is the Domeli thrust fault in eastern Potwar. This Domeli thrust is predicted to be a foreland-verging thrust that demonstrates a great deal of shortening. Potwar is limited by the Domeli thrust in the east [22]. In eastern Potwar, the Domeli back thrust can be observed. No other obstructed back thrust in any sub-district of Potwar is greater in size than the Domeli back thrust. The structure present in the Rajian area is a fault-limited anticline. Other fundamental structural faults compensate their separation level that occurs in Precambrian salt. The Potwar Plateau involves disturbed landscapes. The sub-basin of Potwar is structurally arranged to the south of the western lower regions of the Himalayas and falls in the Potwar Plateau. The Main Boundary Thrust (MBT) limits the basin in the north and toward the east it is limited by the Jhelum left lateral strike slip fault, by the salt range thrust toward the south, and by the Kalabagh right lateral strike slip fault toward the west. Fundamentally, the Potwar sub-basin is unpredictable, and surface structures do not truly mirror the subsurface structures [19].

3. Stratigraphy of the Study Area

The Potwar basin is composed of thick Precambrian evaporate deposits, above which medium to thin Cambrian to Eocene deposits are present, which are further overlain by thick Miocene–Pliocene molasses deposits (Figure 2). The salt lies over the SRT basement, and the thick sand sequence is preserved. The Kussak, Jutana, and Baghanwala Formations are composed of sandstone, siltstone, shales, and dolomites. The whole stratigraphic sequence was interrupted by a few unconformities, and the sequence was highly deformed during Himalayan collision in the Pliocene to Pleistocene period [23].

Three major unconformities reported in the study area are Carboniferous to Ordovician, Mesozoic to Paleocene, and the Oligocene age. During the period of Ordovician to Carboniferous, the Potwar basin uplift began, which is why the sedimentation ceased during this time period. The salt range formation of the Pre-Cambrian age is the oldest formation present here, composed mostly of halite with subordinate marl, dolomite, and shale. This salt range formation lies unconformably over the basement. The overlying sedimentary column includes Eocene to Cambrian shallow marine facies with major unconformities found in the age of Permian and Paleocene. The second major unconformity present in the region, among which no sediment deposition is observed, is the Mesozoic age. In the Mesozoic age, the epicenter area was the central Potwar basin, where thick sedimentary succession of Mesozoic age is preserved. The third major unconformity found is Oligocene age unconformity, where no sedimentary record can be found [19].

The Rajian area is composed of large petroleum deposits, and the petroleum system is well established here. In a subduction association complex, the fore arc area/basins have the best probability of discovering hydrocarbons in huge amount for commercial use. A precise foreland basin (Kohat–Potwar) in a significant part of the Himalayan chain in Pakistan has proved to be the foremost productive region for the discovery of hydrocarbons. The Paleocene Patala shales are considered the most productive wellspring of hydrocarbon in the Potwar basin. Fractured limestone of the Sakesar Formation (Eocene age) and Lockhart Formation (Paleocene age), arenaceous rock of the Tobra Formation (Permian age), and Khewra sandstone (early Cambrian age) are the conceivable reservoir rocks in the Potwar basin. Within the investigation region, the reservoir zone is Chorgali. To seal the leakage of hydrocarbons, drainage, further hydrocarbon migration, and the presence of an impermeable rock layer are fundamental. Fine-grained rocks, for example, shales, evaporate and claystone acts as a compelling top cap rock. In the study region, the Murree Formation of Miocene age provides the hydrocarbons with a seal. Meanwhile, the Dandot and Kussak Formations are also conceivable seal rocks. The petroleum system of the study area is shown in Table 1 [24–26].

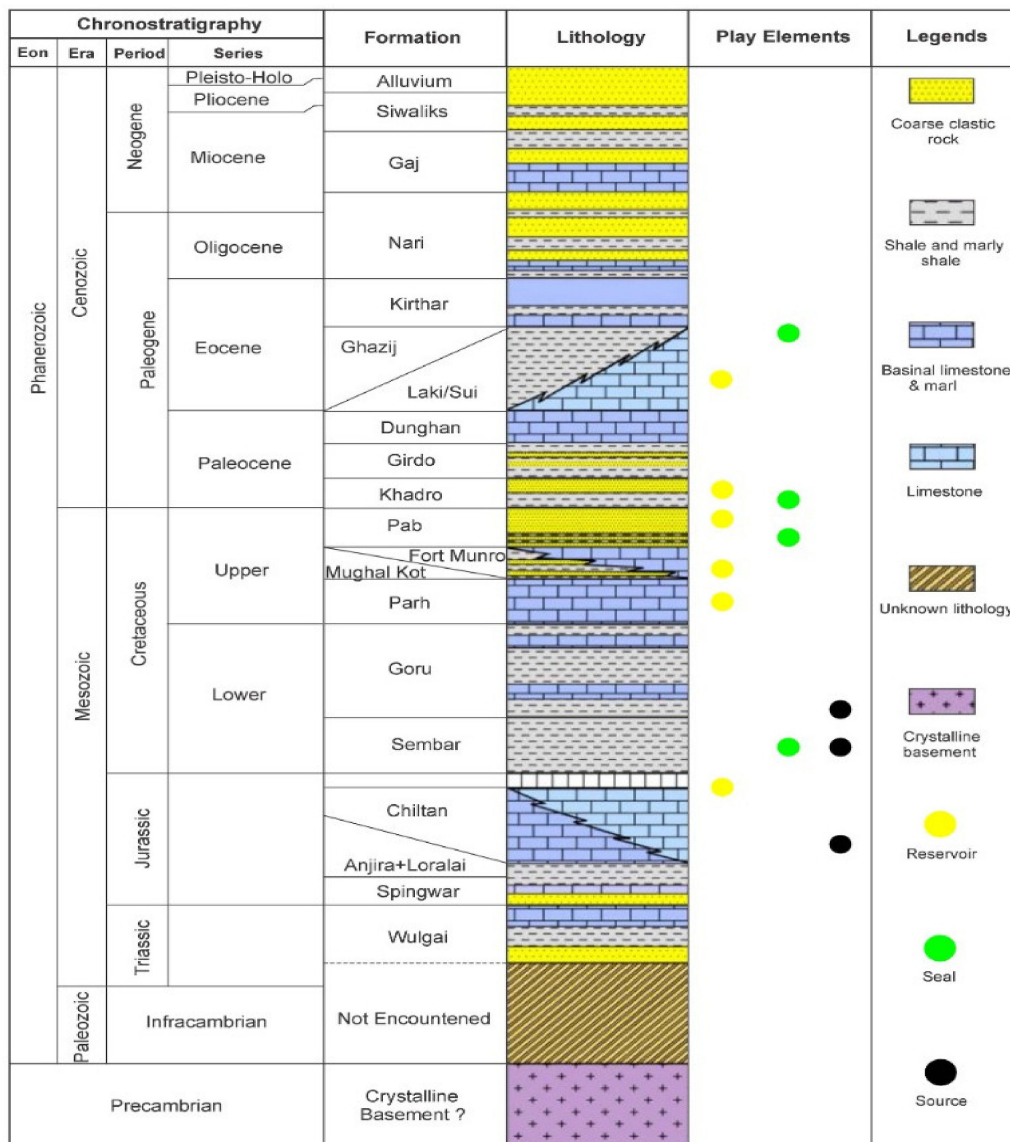


Figure 2. Stratigraphic column of eastern Potwar [22].

Table 1. Petroleum system of the study area.

Formation	Age	Rock Type
Murree, Salt Range	Miocene, Eocene	Seal
Chorgali, Sakesar Limestone	Eocene	Reservoir
Patala, Lockhart Limestone	Paleocene	Source

4. Seismic Data Interpretation

To delineate the subsurface structure of the Rajian area, seismic data interpretation techniques were used. The main purpose of using seismic data interpretation was to discover the potential hydrocarbon traps. The geological conditions of the study area are helpful in delineating the major structural traps. The reflection time was calculated to determine the reflector geometry in this study. Most commonly, structural traps (rather than depths) that tend to contain hydrocarbons are searched here. The two-way-travel (TWT) time is mostly used to interpret the subsurface structure. To display the geometry of selected reflection events, time structural maps are created. A few images in the provided seismic sections can be interpreted easily, but deviations from the regular pattern correspond to areas of structural complications. The most common approach to seismic data interpretation

reveals discontinuous reflections as faults and undulating reflections as folds. This method was selected to identify different seismic facies and their characteristics; to facilitate the dissemination of information regarding the environment of deposition and characteristics of reflection variations; and to identify the stratigraphy and HC potential. Changes in the values of amplitude, frequency, and phase within the waveform are indications of organic compound accretions. Amplitude variation with offset additionally indicates the presence of hydrocarbons. The amendment in the drainage area marking unconformities is useful in the development of depositional surroundings.

4.1. Structural Interpretation

For the structural investigation of the Rajian area through seismic interpretation, the six seismic lines given in Table 2 were used. These six seismic lines consists of five dip lines and one strike line. Using Kingdom software version 2019 by Seismic Micro-Technology (SMT) (Houston, TX, United States), a base map was constructed to show the orientation of these six lines, which ultimately helped in selecting the control line (Figure 3). By interpreting these lines, the changes in structure were observed. The Rajian area is present in a tectonically active (compressional) regime, so the structures observed are mainly the result of compressional forces. Thrust faults, popup structures, duplex geometry, horses, and triangular zones were interpreted in the study area.

Table 2. Seismic lines available for interpretation of the Rajian area.

No.	Line Name	Line Type	Orientation
1.	GO-932-GJN-29	Dip Line	NW–SE
2.	GO-942-GJN-48	Dip Line	NW–SE
3.	GO-932-GJN-12	Dip Line	NW–SE
4.	GO-932-GJN-34	Dip Line	NW–SE
5.	GO-925-GJN-11	Dip Line	NW–SE
6.	GO-942-GJN-50	Strike Line	NE–SW

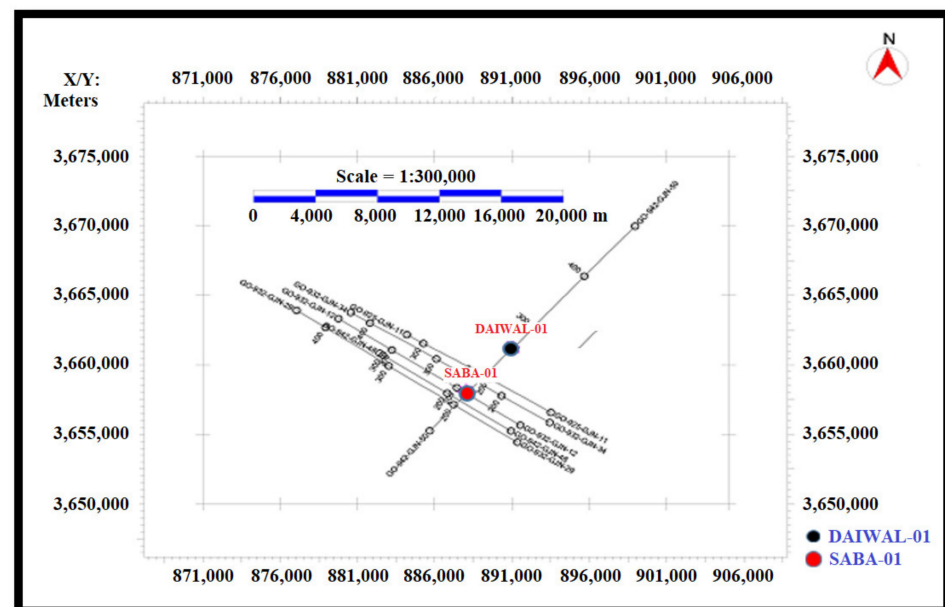


Figure 3. Base map of the Rajian area showing Saba-01 and Daiwal-01 wells.

4.2. Seismic to Well Tie

After the selection of the control line, the velocity window that is closer to SP 175 is resolved. The velocity window depicts the information regarding time (in milliseconds)

and its respective RMS (Root Mean Square) velocity. By using the formula given below for each time, depth is calculated.

$$\text{Depth} = \text{Velocity} \times \text{Time} / 2000$$

The time depth (TD) chart in Figure 4 was built using depth found by resolving two velocity windows along with the time. Time is plotted on the y -axis, whereas depth is plotted on the x -axis. The information required for finding the formation depth was extracted from well top data. The time and point on the control point were then calculated, where the concerned reflectors were present to mark the horizons. The formation's top depth from kelly bushing (KB), values of KB in the well top data, and SRD are given in the seismic sections. As the depth was taken with reference to KB, it needed to be converted into seismic reference datum (SRD) to place it on the available seismic lines. This is known as the seismic to well tie [27].

$$\text{Formation Depth} = \text{Formation Top depth from KB} - \text{Kelly Bushing} + \text{SRD}$$

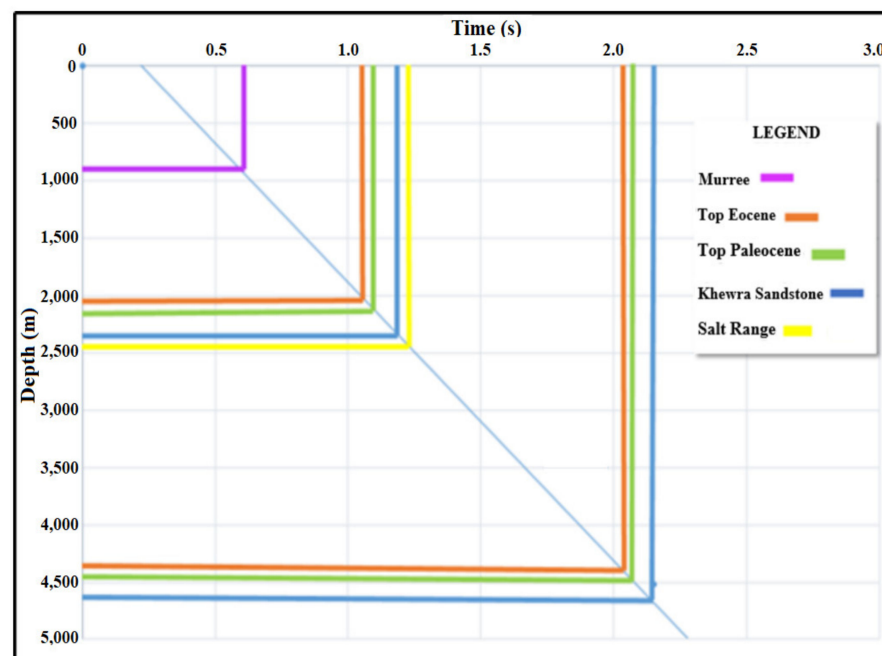


Figure 4. Time depth (TD) chart.

In the current study, three packages were marked on the control line (Table 3). The first package consists of the Murree Formation, top Eocene (Nammal, Sakesar, and Chorgali), top Paleocene (Hangu, Lockhart, and Patala), Khewra sandstone, and the salt range. Package 2 consists of top Eocene, top Paleocene, and Khewra sandstone. Package 3 is the same as package 2 but is marked at a deeper depth by referring to the model constructed in packages 1 and 2. After the marking of traces on our control line (942-JN-50), jump correlation was used to mark and extend reflectors to the bounds of the seismic section. Once a strike line was marked with all of the reflectors, the reflectors were marked on the five provided dip lines, namely, 932GJN-29, 942-GJN-48, 932-GJN-12, 932-GJN-34, and 925-GJN-11, using the loop time method.

Table 3. Marking of horizons on control line through well to seismic tie.

Formation Name	Formation Depth = Formation Top – Kelly bushing + SRD	Formation Depth (m)	Two Way Time (seconds)	Well Name
Murree 1 Formation	FD = 1079 – 513 + 350	916	0.55	Saba-01
Top Eocene 1	FD = 2215 – 513 + 350	2052	1.17	Saba-01
Top Paleocene 1	FD = 2337 – 513 + 350	2174	1.24	Saba-01
Khewra Sandstone 1	FD = 2526 – 513 + 350	2363	1.32	Saba-01
Salt Range	FD = 2654 – 513 + 350	2491	1.39	Saba-01
Top Eocene 2	FD = 4587 – 577 + 350	4360	2.07	Daiwal-01
Top Paleocene 2	FD = 4700 – 577 + 350	4473	2.12	Daiwal-01
Khewra Sandstone 2	FD = 4890 – 577 + 350	4663	2.18	Daiwal-01

4.3. Fault Marking and Interpretation

Based on the break in continuity, faults were marked on all dip lines. The current study area lies in the eastern part of the Potwar Plateau, with northward dipping strata and local open folds of low structural relief and axes. In addition to these clearly plotted major and minor faults, there are a number of minor faults present in the area whose structural importance was somewhat ambiguous (Table 4). Rajian is a structure formed by the grouping of thrusts (SRT and Dil jabba) and a back thrust (Domeli), forming a triangular zone in the subsurface. Saba-01 is drilled on the strike line at shot point 175. However, for better understanding of the structural complexities of the subsurface, the well tops of Daiwal-01 well drilled at shot point 260 on the same strike line were used.

Table 4. Major and minor faults marked on seismic sections.

Fault Name	Fault Nature	Tectonic Transport Direction
Major Fault (F1)	Basement Thrust	SE
Major Fault (F2)	Major Thrust	SE
Major Fault (F3)	Roof Thrust	SE
Major Fault (F4)	Back Thrust	NW
Minor Fault (f1)	Thrust	SE
Minor Fault (f2)	Thrust	SE
Minor Fault (f3)	Thrust	SE
Minor Fault (f4)	Thrust	SE
Minor Fault (f5)	Thrust	SE

4.4. Horizon Marking and Interpretation

The target horizons were picked up across seismic lines after the identification of the horizons when the reflectors changed their character from high to low amplitude. Interpretation was performed on the basis of the difference in the acoustic impedance or thickening or thinning of the different formations. The horizons were selected along all of the seismic girds by correlating the seismic events. In Figure 5a, the line 942-GJN-50 is oriented in the NE–SW direction, perpendicular to the dip of the major faults, and parallel to the axis of the structure present in the area. Two packages were encountered on the strike line. Package 1 is composed of the Murree Formation, top Eocene, top Paleocene, Khewra sandstone, and the salt range formation. Package 2 is composed of top Eocene, top Paleocene, and Khewra sandstone. Saba-01 is drilled at SP 175 on the SW flank, and Daiwal-01 is drilled at SP 230 on the SE flank.

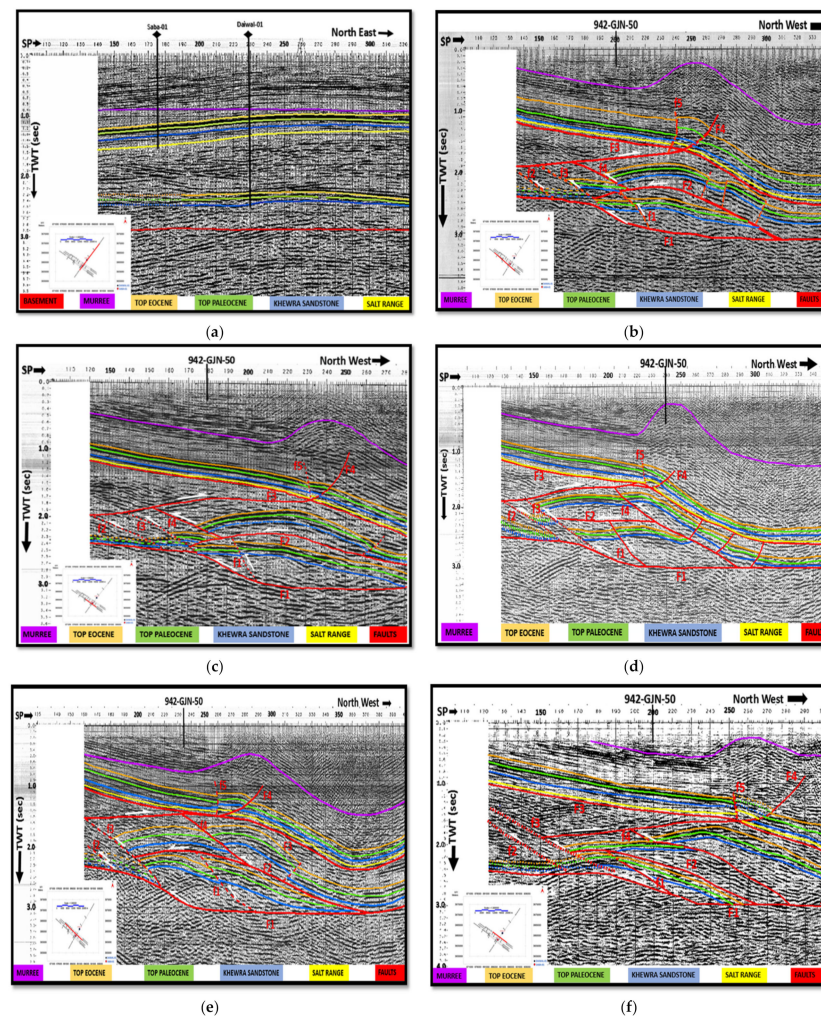


Figure 5. Interpretation of the seismic lines: (a) 942-GJN-50 line, (b) 942-GJN-29 line, (c) 942-GJN-48 line, (d) 932-GJN-12 line, (e) 932-GJN-34 line, and (f) GO-925-GJN-11 line.

In Figure 5b, the line 932-GJN-29 is oriented in the northwest direction and is to the west of Saba-01 and Daiwal-01. The salt range provides the detachment zone and is responsible for generating two major faults in the area: the fore thrust and back thrust. All the major and minor faults are visible on this seismic line. In Figure 5c, line 942-GJN-48 is located to the west of Saba-01 and Daiwal-01 wells and is oriented in the NW direction. No well has been drilled on this line. It can be observed from the structures that the back thrust is SE verging and the roof thrust is NW verging. Minor faults create localized positive geometries in between the major thrusts.

In Figure 5d, the seismic line 932-GJN-12 is situated to the west of Saba-01 and Daiwal-01 wells. The structures displayed in this section are similar to those shown in Figure 5c for line 942-GJN-48. In Figure 5e, line 932-GJN-34 is situated to the west of Saba-01 and Daiwal-01 well. It also shows a triangular zone formed by a back thrust and roof thrust. Both of the thrusts die out in the Siwaliks group. This line shows the NW extension of the structure as observed in the previous sections.

In fold and thrust belt areas, structural features named triangular zones are characterized by complex layer geometry and velocity variations. The poor quality of the seismic image encountered in such geological settings is due to the complex propagation of seismic energy through the overburden structure associated with strong velocity distribution. It results in shadow zones and in geometrically deformed seismic events, which make interpretation difficult. In order to select the seismic processing parameters such as migration velocities and reduce the ambiguities in structural interpretation, it is important to better

understand the real seismic wave propagation for these specific seismic events that we can clearly see in the seismic section (Figure 5f). Velocity models were built and introduced into the Kingdom software version 2019 by Seismic Micro-Technology (SMT) (Houston, TX, United States). Using non-zero and zero-offset ray tracing modelling, seismic interpretation was carried out to analyze specific seismic travel paths encountered in these areas. We demonstrated that these events could be generated by complex seismic wave propagation, which leads to ambiguities in time seismic sections (Figure 5f). As specific artefacts such as pull-up and shadow zone effects are present in Figure 5f, the line 925-GJN-11 is present to the west of Saba-01 and Daiwal-01 wells. The major structural framework in all the dip lines is the same, consisting of four major thrust faults; in between these, there are a number of minor faults. The Rajian area is in the region of the Potwar basin where the presence of a triangular zone has been confirmed, and the direction of thrust sheets in our area of interest also suggested its presence. The minor faults cut into the rock packages and give them localized positive geometries. A large number of clear and ambiguous splay faults are also present here.

The interpretation of various dip lines shows that the strata continuation has been disturbed by faulting. Four major faults in addition to minor faults were observed. F3 is the roof thrust dipping in the NW direction. F4 is the back thrust dipping in the SE direction. The hanging wall has moved upward relative to the foot wall, and, therefore, higher values of time are noted for the foot wall. F3 shows greater throw when compared to that of F4. The combination of a back thrust and salt range thrust, also called roof thrust (bounding the strata from below), results in the formation of a structure known as the triangular zone. The other two major faults (F1 and F2) are present in the lower package and regard the strata uplift in the same manner as that of F3 and F4. F1 acts as a major thrust dipping in the NW direction and bounding the second package in the subsurface. Fault F1 is essentially the basement or floor thrust, below which the zone of interest is absent.

5. Contour Maps

The structural and stratigraphic configuration of the subsurface was performed using TWT and depth contour maps. The results of seismic interpretation are represented in contours maps; that is, the three-dimensional earth surface is represented in dimensions using contouring. Kingdom software version 2019 by Seismic Micro-Technology (SMT) (Houston, TX, United States) was used for the construction of contour maps.

Time and Depth Contour Maps

The time contour maps show the contour lines with the same values of time. They represent the two-way travel time. The values are plotted on the base where the information of latitude and longitude is already present. For the interpretation of an area, more than one section of seismic data is required for the same area. The contour interval for top Eocene 1, top Paleocene 1, Khewra sandstone, and the salt range is 0.05 s. Similarly, the time contour interval for top Eocene 2 and Paleocene 2 is also 0.05 s. The darker the color, the greater the values of time and the deeper it is, whereas the lighter the color, the lower the time values and the shallower it is. The time values are low in the anticlines along the core, while they are high along the flanks. In the synclines, the time values are high along the core but low along the flanks. All of this information was interpreted using contour maps.

The time contour maps of shallower rock package, i.e., top Eocene 1 (Figure 6a), top Paleocene 1 (Figure 6b), Khewra sandstone 1 (Figure 6c), and salt range 1 (Figure 6d) show the change in elevation from east to west. The contour's arrangement shows the deepening of the first package toward the west. The package is cut by a major thrust (F4), as shown in Figure 6. There is also the presence of a minor fault in the same package, and this minor fault has a very minor structural influence on the rock package. The time contour maps of the second package (Figure 6e,f) show that the package is bounded above by the roof

thrust (F3) and below by a major thrust (F2). These two thrusts bind the anticlinal package and provide it with the sealing effect. Three minor faults cut the package and change its smooth dipping from east to west.

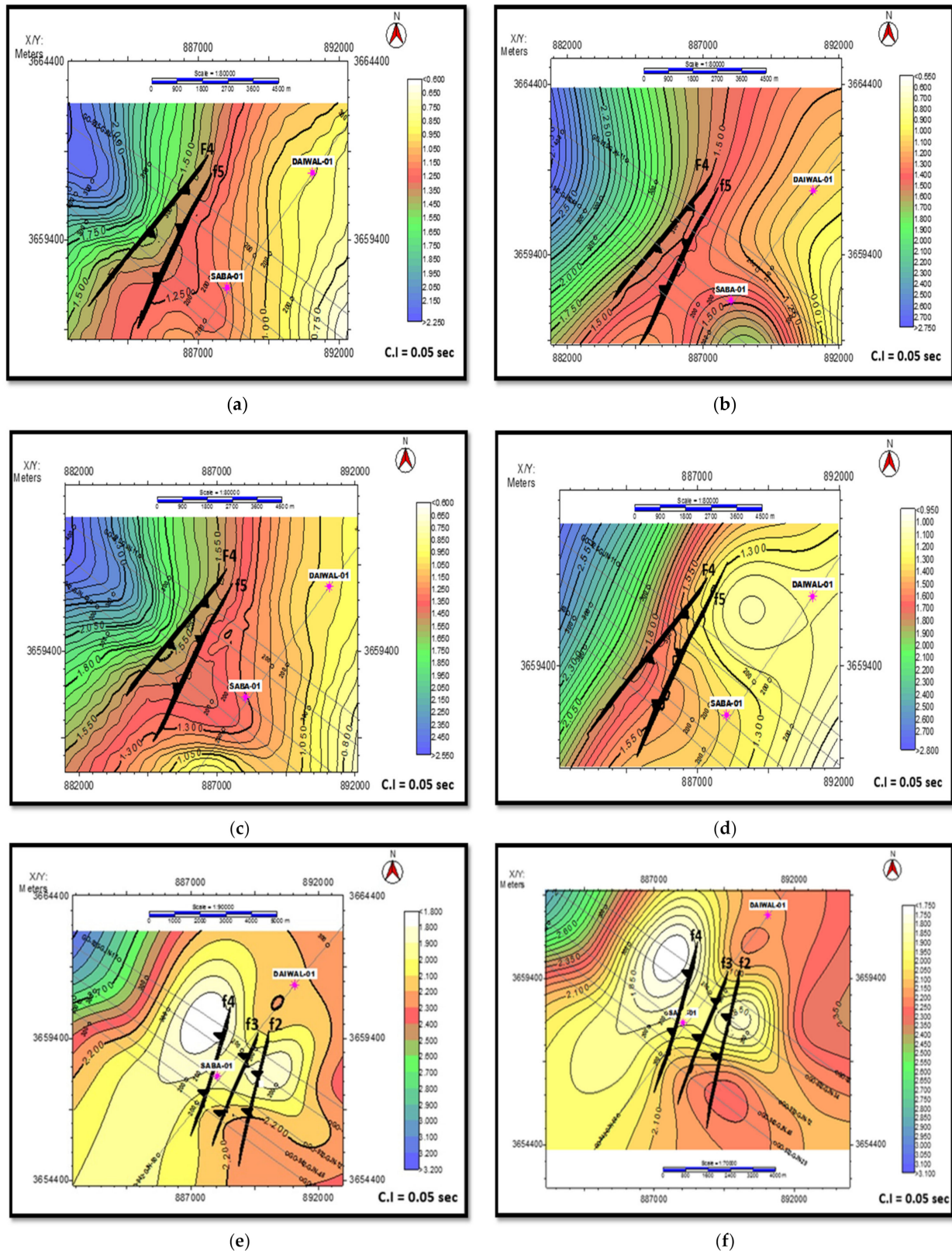


Figure 6. Time contour maps for Contour Interval (C.I) of 0.05 sec, for (a) top Eocene 1, (b) top Paleocene 1, (c) Khewra sandstone 1, (d) walt range 1, (e) top Eocene 2, and (f) top Paleocene 2.

Depth contour maps mainly show the depth of underlying strata and the structures. Faults, anticlines, and folds are usually portrayed by depth contour maps. Their interpretation is similar to that for contour maps of time. This allows for correct information regarding the structure style in the subsurface to be obtained. With the help of these depth and TWT contour maps, it can be concluded that Eocene age formations and Khewra sandstone are the reservoir rocks of the Rajian area. The depth contour maps of the shallow rock package are top Eocene 1 (Figure 7a), top Paleocene 1 (Figure 7b), Khewra sandstone 1 (Figure 7c), and salt range 1 (Figure 7d). The depth contour maps of top Eocene 2 (Figure 7e) and top Paleocene 2 (Figure 7f) were constructed with a contour break of 250 m. These maps for top Paleocene, top Eocene, and Khewra sandstone show that the Khewra Formation is deeper than the other two marked formations. While moving from blue to white color, the structure becomes shallower, indicating that the structure is changing from syncline to anticline.

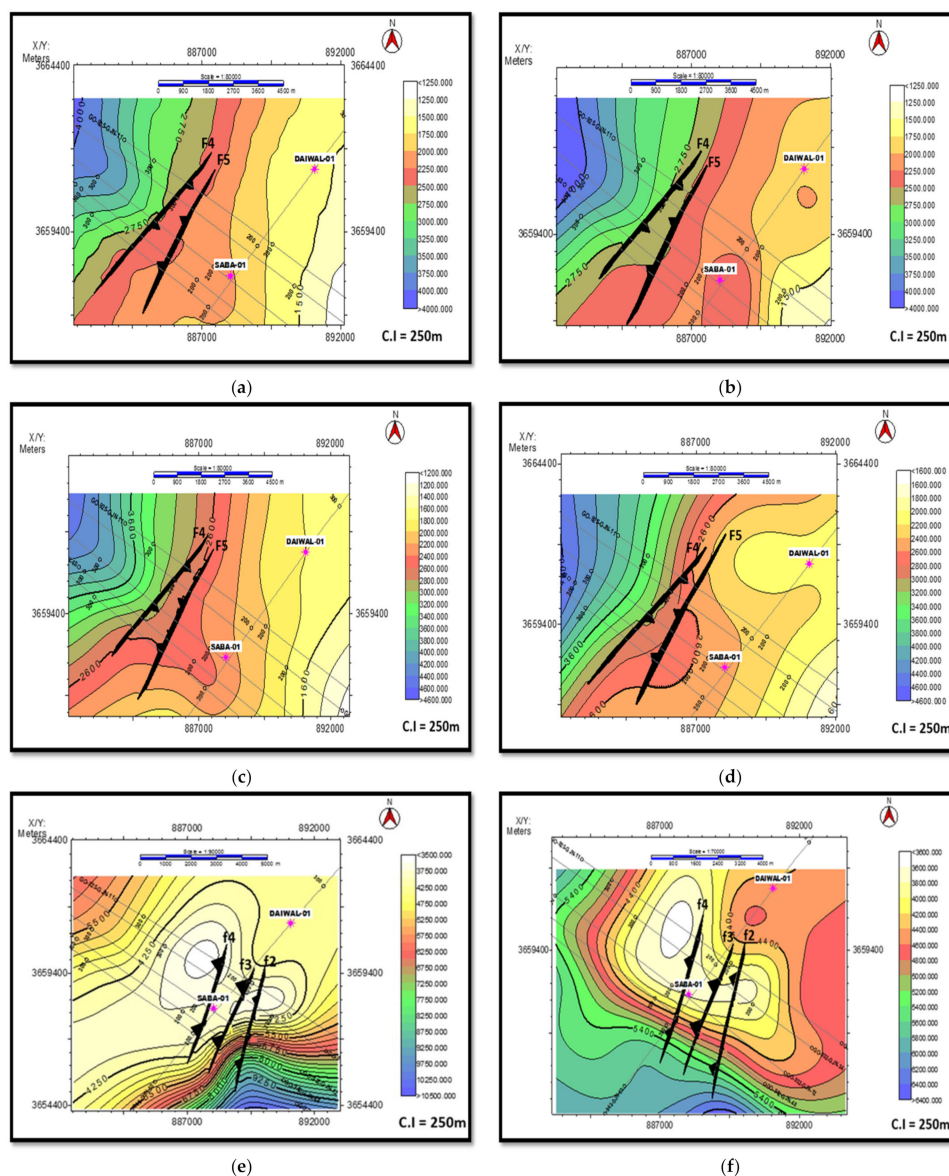


Figure 7. Depth contour maps for Contour Interval (C.I) of 250 m, for (a) top Eocene 1, (b) top Paleocene 1, (c) Khewra sandstone 1, (d) salt range 1, (e) top Eocene 2, and (f) top Paleocene 2.

Both types of contour maps (time and depth) represent the subsurface structural arrangement. Only those faults that are cutting the formations and producing localized

structural changes in the whole package are displayed in the contour maps. However, the two packages are bounded by major thrust faults as discussed thoroughly in seismic interpretation of the given lines.

6. Petrophysical Analysis

Petrophysics is a method that is used to describe the reservoir, and it helps in the identification and quantification of a fluid in a reservoir. By using wireline logs (density, neutron, self-potential, and resistivity), petrophysical analysis was performed for one zone in Saba-01. The analyses were performed to calculate porosity, water resistivity, water saturation, and oil saturation, which are used to identify the hydrocarbon potential of the reservoir. Three types of wireline logs were used (Table 5) to carry out reservoir analysis. Due to the unavailability of the well tops of the lower sheet of Saba-01 well, a gamma ray log was used to identify a clean zone (Table 6).

Table 5. Logs available for petrophysical interpretation of reservoir zones.

Lithological Logs	Porosity Logs	Fluid Dynamic Logs
Gamma Ray Log (GR)	Sonic Log (DT)	Resistivity Logs (LLD and LLS)
Self-Potential Log (SP)	Density Log (RHOB)	-
-	Neutron Log (NPHi)	-

Table 6. Potential zones for hydrocarbon accumulation.

ZONE 1	
Initial Depth (m)	3740
End Depth (m)	3835
Thickness (m)	95
ZONE 2	
Initial Depth (m)	4015
End Depth (m)	4100
Thickness (m)	85

6.1. Interpreting the Hydrocarbon-Bearing Zone

For the interpretation of the hydrocarbon-bearing zone (thought to be potential), the following methodology was adopted:

1. Calculation of the volume of shale (Vsh);
2. Calculation of the volume of clean (Vclean);
3. Calculation of density porosity (DPHI);
4. Calculation of neutron porosity (NPHI);
5. Calculation of average porosity (APHI);
6. Calculation of effective porosity (EPHI) and sonic porosity (SPHI);
7. Calculation of the resistivity of water (Rw);
8. Calculation of water saturation (Sw);
9. Calculation of hydrocarbon saturation (Sh).

6.1.1. Petrophysical Interpretation of Reservoir Zone 1

The results obtained from all of these steps (Table 7) indicate that the hydrocarbon saturation of the zone is 11%. This hydrocarbon saturation percentage is satisfactory for exploratory purposes. However, the discovery is highly dependent on economics. Figure 8a shows the variation in volume of shale with respect to the depth of zone 1. Altogether, the trend of the volume of shale is on the lower side. The clean zone indicates the zone that represents the potential for hydrocarbon reserves. The average value of Vsh is 23.35%. The maximum value Vsh can be observed at a depth of 3832 m.

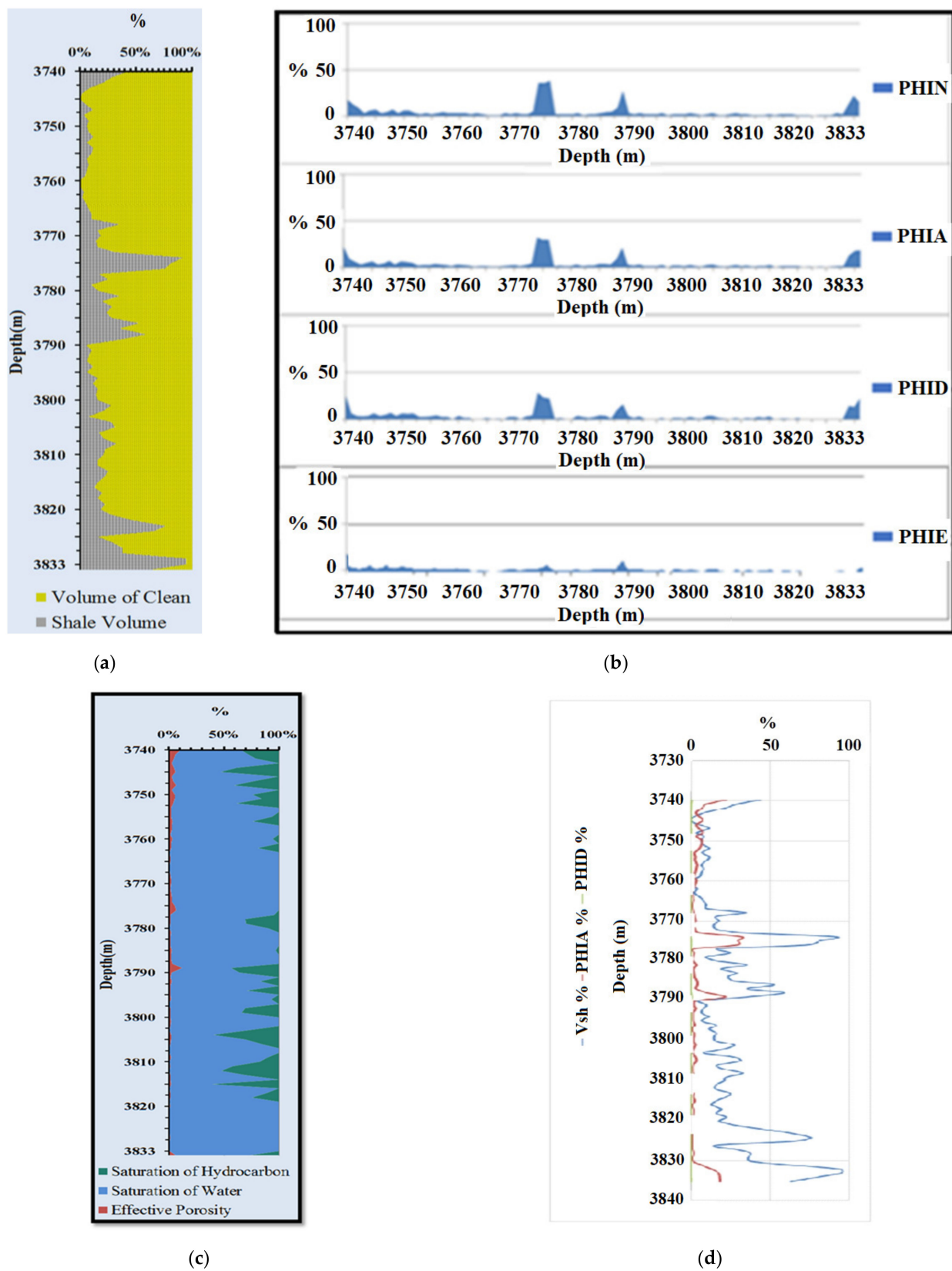


Figure 8. (a) Relationship between the volume of shale and volume of clean with respect to the depth of zone 1; (b) relationship between neutron porosity, average porosity, density porosity, and effective porosity of zone 1; (c) Relationship between the saturation of water and saturation of hydrocarbon for zone 1; (d) relationship between the volume of shale (Vsh), average porosity (PHIA), and average density porosity (PHID) of zone 1.

Table 7. Petrophysical analysis results obtained for zone 1.

Zone 1	
Depth (m)	3740 to 3835
Thickness (m)	95
Average Vsh (%)	23.35
Average Vclean (%)	76.64
Average Density Porosity (PHID) (%)	3.92
Average Neutron Porosity (PHIN) (%)	4.69
Average Porosity (PHIA) (%)	4.30
Average Effective Porosity (PHIE) (%)	2.42
Average Water Saturation (Sw) (%)	88.09
Average Hydrocarbon Saturation (Sh) (%)	11.9

Figure 8b shows the variation in neutron porosity, average porosity, density porosity, and effective porosity with respect to depth. The average value of neutron porosity is 4.69%; the average porosity is 4.30%; the density porosity is 3.92%; and the effective porosity is 2.42%. In Figure 8c, the variation in water saturation and hydrocarbon saturation according to depth is presented. Average hydrocarbon saturation is about 11.09% and average water saturation is about 88.09%. In Figure 8d, the variation in average porosity and effective porosity can be seen with respect to depth. The effective porosity average value is 2.3%; the volume of the shale average value is 23.35%; and average value of average porosity is 4.1%. The effective porosity indicates the amount of connected pore spaces.

6.1.2. Petrophysical Interpretation of Reservoir Zone 2

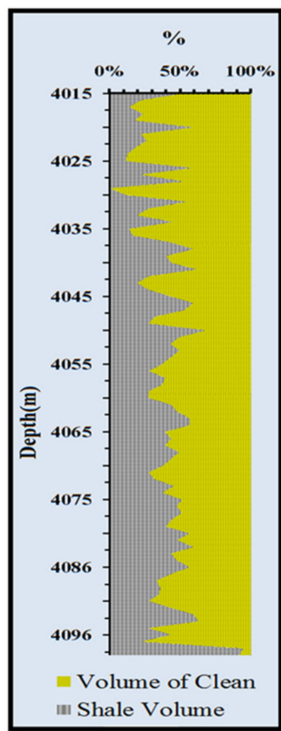
Table 8 summarizes the petrophysical interpretation of reservoir zone 2. Figure 9a shows the variation in the volume of shale with respect to the depth of zone 2. The average value of shale is 39.9%. The maximum value of the volume of shale can be observed at the depth of 4098 m. The maximum value of clean lithology can be observed at 4029 m and its minimum value at 4098 m. In Figure 9b, the variation in neutron porosity, average porosity, density porosity, and effective porosity with respect to depth can be observed. The average value of neutron porosity is 8.8%; average porosity is 8.79%; density porosity is 8.70%; and effective porosity is 5.64%.

Table 8. Petrophysical interpretation of reservoir zone 2.

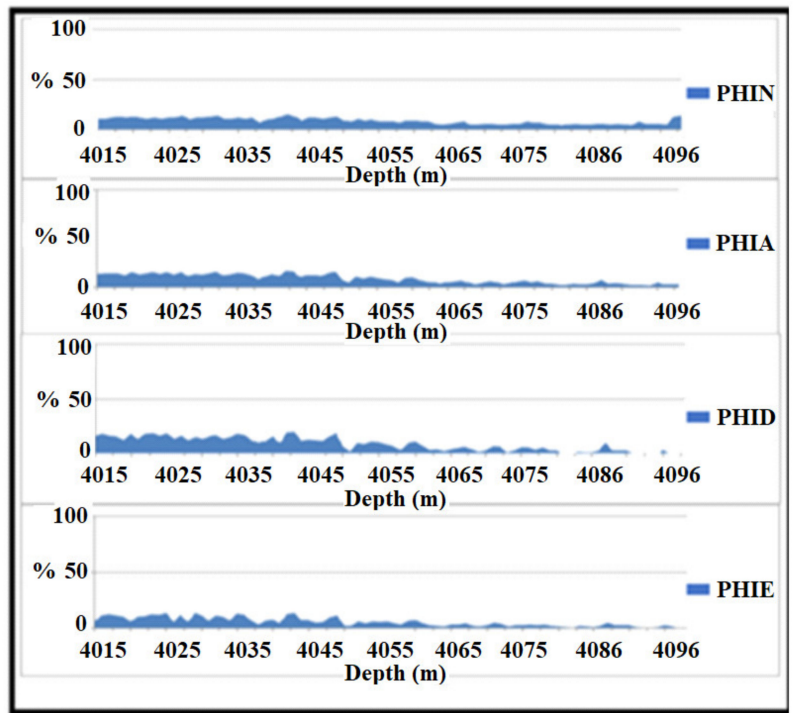
Zone 2	
Depth (m)	4015 to 4100
Thickness (m)	85
Average Vsh (%)	39.98
Average Vclean (%)	60.01
Average Density Porosity (PHID) (%)	8.70
Average Neutron Porosity (PHIN) (%)	8.89
Average Porosity (PHIA) (%)	8.79
Average Effective Porosity (PHIE) (%)	5.64
Average Water Saturation (Sw) (%)	100
Average Hydrocarbon Saturation (Sh) (%)	0

In Figure 9c, the variation in average porosity and effective porosity with respect to depth can be observed. Average porosity's average value is 16%; effective porosity's average value is 11.6%; and sonic porosity's average value is 9.4%. Figure 9d shows variation in water saturation and hydrocarbon saturation with respect to depth. Average hydrocarbon saturation is about 0%, and average water saturation is about 100%.

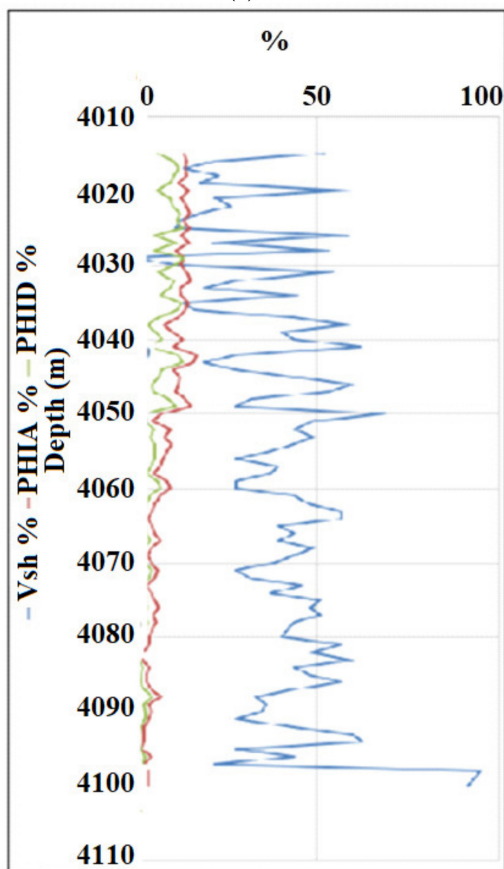
From all of the graphs presented above, it is clear that zone 1 has 11.09% hydrocarbon saturation, while zone 2 has 100% water saturation. All of the curve trends confirm these results.



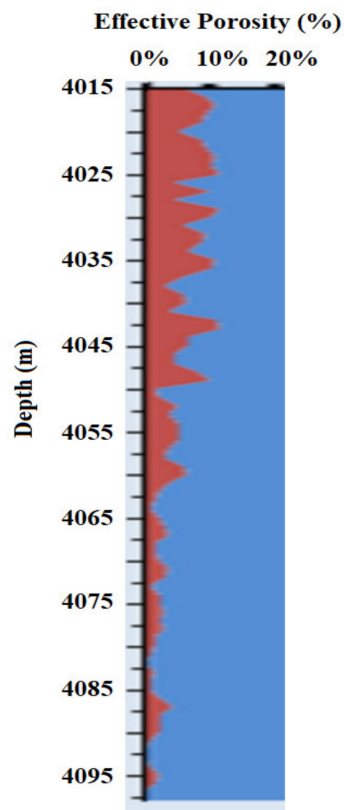
(a)



(b)



(c)



(d)

Figure 9. (a) Relationship between volume of shale and volume of clean with respect to the depth of zone 2; (b) relationship between neutron porosity, average porosity, density porosity, and effective porosity of zone 2; (c) relationship between the volume of shale (Vsh), average porosity (PHIA), and average density porosity (PHID) of zone 2; (d) variation in effective porosity along the depth.

7. Conclusions

The objective of the current research was to interpret the subsurface structural features of the Rajian area, Upper Indus Basin, Pakistan, using 2D seismic sections and identification of hydrocarbon-bearing zones using petrophysical analysis. The main outcomes of the study are summarized as follows:

- The presence of reverse (thrust) faults indicates that the Rajian area lies in a compressional regime.
- Seismic data interpretation shows that the Rajian oil field has a triangular zone structure formed by a major thrust that dips in the NW direction, while the back thrust dips in the SE direction.
- The overall structure presented in the study area supports a duplex geometry, where the salt range thrust acts as a floor thrust and the roof thrust is a back thrust marking a passive roof duplex.
- The package bounded by roof and floor thrusts is bisected by several low angle thrust faults (imbrications) presenting the phenomenon of horizontal stacking, which, in turn, shows intense shortening in the area.
- Time and depth contour maps of top Eocene and top Paleocene formations helped us to confirm the presence of positive structures in the area. The time contour maps for the first package show the change in elevation from east to west. The contour's arrangement shows the deepening of the first package toward the west. The package is cut by a major thrust (F4). There is also the presence of a minor fault in the same package, but this minor fault has a very minor structural influence on the rock package. Time contour maps of the second package show that the package is bounded above by the roof thrust (F3) and below by a major thrust (F2). These two thrusts bind the anticlinal package and provide it with a sealing effect. Three minor faults cut the package and change its smooth dipping from east to west.
- Petrophysical analysis performed on one zone of saba-01 suggests that hydrocarbon saturation in zone 1 is about 11.09%. The hydrocarbon saturation percentage in zone 1 is sufficient to be considered for future oil and gas production. The petrophysical analysis of zone 2 suggests negligible traces of the hydrocarbon, and, as such, zone 2 should not be considered for future oil and gas production. Based on the petrophysical analysis performed in this study, the water saturation is 100% in zone 2; thus, it can be used as a potential CO₂ sequestration site.

Author Contributions: Conceptualization, N.A., S.K., E.F.N., Z.Z. and A.A.-S.; methodology, N.A., S.K., E.F.N., Z.Z. and A.A.-S.; software, N.A., S.K. and E.F.N.; validation, N.A., S.K., E.F.N., Z.Z. and A.A.-S.; formal analysis, N.A., S.K., E.F.N. and A.A.-S.; investigation, N.A., S.K. and A.A.-S.; resources, N.A., S.K. and A.A.-S.; data curation, N.A., S.K. and A.A.-S.; writing—original draft preparation, N.A., S.K., E.F.N., Z.Z. and A.A.-S.; writing—review and editing, N.A., S.K. and A.A.-S.; visualization, N.A., S.K., E.F.N., Z.Z. and A.A.-S. All authors have read and agreed to the published version of the manuscript.

Funding: This research received funding from the College of Petroleum Engineering and Geosciences of KFUPM through Startup Fund grant number SF 18060.

Data Availability Statement: The data presented in this study are available upon request from the corresponding author.

Acknowledgments: The authors appreciate and acknowledge the support provided by King Fahd University of Petroleum and Minerals (KFUPM) for providing all the essential resources for conducting this study.

Conflicts of Interest: The authors declare no conflict of interest.

References

1. Ahmad, N.; Khan, S.; Al-Shuhail, A. Seismic Data Interpretation and Petrophysical Analysis of Kabirwala Area Tola (01) Well, Central Indus Basin, Pakistan. *Appl. Sci.* **2021**, *11*, 2911. [[CrossRef](#)]

2. Khan, A.M.; Al-Juhani, S.G.; Abdul, S. Digital Viscoelastic Seismic Models and Data Sets Of Central Saudi Arabia in the Presence of Near-Surface Karst Features. *J. Seism. Explor.* **2020**, *29*, 15–28.
3. Chan, S.A.; Edigbue, P.; Khan, S.; Ashadi, A.L.; Al-Shuhail, A.A. Viscoelastic Model and Synthetic Seismic Data of Eastern Rub'Al-Khali. *Appl. Sci.* **2021**, *11*, 1401. [[CrossRef](#)]
4. A Study on Multiple Time-Lapse Seismic AVO Inversion—LI—2005—Chinese Journal of Geophysics Wiley Online Library. Available online: <https://agupubs.onlinelibrary.wiley.com/doi/abs/10.1002/cjg2.738> (accessed on 5 November 2020).
5. Ou, C.; Li, C.; Rui, Z.; Ma, Q. Lithofacies distribution and gas-controlling characteristics of the Wufeng–Longmaxi black shales in the southeastern region of the Sichuan Basin, China. *J. Pet. Sci. Eng.* **2018**, *165*, 269–283. [[CrossRef](#)]
6. Soleimani, M. Seismic imaging by 3D partial CDS method in complex media. *J. Pet. Sci. Eng.* **2016**, *143*, 54–64. [[CrossRef](#)]
7. Parvez, M.K. Petroleum Geology of Kohat-Bannu Plateau, Northwest Frontier Province, Pakistan. Ph.D. Thesis, University of South Carolina, Columbia, SC, USA, 1992.
8. Soleimani, M. Well performance optimization for gas lift operation in a heterogeneous reservoir by fine zonation and different well type integration. *J. Nat. Gas Sci. Eng.* **2017**, *40*, 277–287. [[CrossRef](#)]
9. Al-Shuhail, A.A.; Alshuhail, A.A.; Khulief, Y.A.; Salam, S.A.; Chan, S.A.; Ashadi, A.L.; Al-Lehyani, A.F.; Almubarak, A.M.; Khan, M.Z.U.; Abdulrahman, K.A.; et al. KFUPM Ghawar digital viscoelastic seismic model. *Arab. J. Geosci.* **2019**, *12*, 245. [[CrossRef](#)]
10. Khan, S.; Al-Shuhail, A.A.; Khulief, Y.A. Numerical modeling of the geomechanical behavior of Ghawar Arab-D carbonate petroleum reservoir undergoing CO₂ injection. *Environ. Earth Sci.* **2016**, *75*, 1499. [[CrossRef](#)]
11. Khan, S.; Khulief, Y.A.; Al-Shuhail, A.A. The effect of injection well arrangement on CO₂ injection into carbonate petroleum reservoir. *Int. J. Glob. Warm.* **2018**, *14*, 462–487. [[CrossRef](#)]
12. Khan, S.; Khulief, Y.A.; Al-Shuhail, A.A. Numerical modeling of the geomechanical behavior of Biyadh reservoir undergoing CO₂ injection. *Int. J. Geomech.* **2017**, *17*, 04017039. [[CrossRef](#)]
13. Khan, S.; Khulief, Y.A.; Al-Shuhail, A.A. Reservoir Geomechanical Modeling during CO₂ Injection into Deep Qasim Reservoir: A Study Focused on Mitigating Climate Change. In *World Environmental and Water Resources Congress 2020: Groundwater, Sustainability, Hydro Climate/Climate Change, and Environmental Engineering*; American Society of Civil Engineers: Reston, VA, USA, 2020; pp. 29–40.
14. Garba, M.D.; Muhammad, U.; Khan, S.; Farrukh, K.; Ahmad, S.; Muhamad, G.; Akram, F.E.; Muhammad, H. CO₂ towards fuels: A review of catalytic conversion of carbon dioxide to hydrocarbons. *J. Environ. Chem. Eng.* **2021**, *9*, 104756. [[CrossRef](#)]
15. Israf, U.D.; Usman, M.; Khan, S.; Aasif, H.; Alotaibi, M.A.; Alharthi, A.I.; Centi, G. Prospects for a green methanol thermo-catalytic process from CO₂ by using MOFs based materials: A mini-review. *J. CO₂ Util.* **2021**, *43*, 101361. [[CrossRef](#)]
16. Soleimani, M.; Shokri, B.J.; Rafiei, M. Integrated petrophysical modeling for a strongly heterogeneous and fractured reservoir, Sarvak Formation, SW Iran. *Nat. Resour. Res.* **2017**, *26*, 75–88. [[CrossRef](#)]
17. Radfar, A.; Chakdel, A.R.; Nejati, A.; Soleimani, M. New insights into the structure of the South Caspian Basin from seismic reflection data, Gorgan Plain, Iran. *Int. J. Earth Sci.* **2019**, *108*, 379–402. [[CrossRef](#)]
18. Khan, M.A.; Ahmed, R.; Raza, H.A.; Kemal, A. Geology of petroleum in Kohat-Potwar depression, Pakistan. *AAPG Bull.* **1986**, *70*, 396–414.
19. Riaz, M.; Nuno, P.; Zafar, T.; Ghazi, S. 2D Seismic Interpretation of the Meyal Area, Northern Potwar Deform Zone, Potwar Basin, Pakistan. *Open Geosci.* **2019**, *11*, 1–16. [[CrossRef](#)]
20. Jaumé, S.C.; Lillie, R.J. Mechanics of the Salt Range-Potwar Plateau, Pakistan: A fold-and-thrust belt underlain by evaporites. *Tectonics* **1988**, *7*, 57–71. [[CrossRef](#)]
21. Hussain, W.; Abbas, S.Q.; Hussain, S. Structure Investigation, Economics and Stratigraphy of the Paleozoic, Mesozoic and Cenozoic Sequence in the Vicinity Eastern and Western side of the Salt Range, Punjab Pakistan. *J. Inf. Commun. Technol. Robot. Appl.* **2018**, *6*, 95–116.
22. Qureshi, M.A.; Ghazi, S.; Riaz, M.; Ahmad, S. Geo-seismic model for petroleum plays an assessment of the Zamzama area, Southern Indus Basin, Pakistan. *J. Pet. Explor. Prod. Technol.* **2021**, *11*, 33–44.
23. Khel, B.; Hills, T.; Nilawan, K.R. Surghar Range Soan River 20 40 60 33 N km BANNU Potwar Plateau. In *Earth's Pre-Pleistocene Glacial Record*; University of Rochester: Rochester, NY, USA, 2011; p. 278.
24. Gee, E.R.; Gee, D.G. Overview of the geology and structure of the Salt Range, with observations on related areas of northern Pakistan. *Geol. Soc. Am. Spec. Pap.* **1989**, *232*, 95–112.
25. Ghazi, S.; Ali, A.; Hanif, T.; Sharif, S.; Arif, J. Larger benthic foraminiferal assemblage from the Early Eocene Chor Gali Formation, Salt Range, Pakistan. *Geol. Bull. Punjab Univ.* **2010**, *45*, 8391.
26. Sameeni, S.J.; Nazir, N.; Abdul-Karim, A.; Naz, H. Foraminiferal biostratigraphy and reconnaissance microfacies of Paleocene Lockhart Limestone of Jabri area, Hazara, northern Pakistan. *Geol. Bull. Punjab Univ.* **2009**, *44*, 85–96.
27. Margrave, G.F. Why Seismic-to-Well Ties Are Difficult. 25th Annual Report of the CREWES Project 2013. Available online: <https://www.crewes.org/Documents/ResearchReports/2013/CRR201359.pdf> (accessed on 10 August 2021).